MATERIALE PLASTICE
https://revmaterialeplastice.ro
https://doi.org/10.37358/Mat.Plast.1964

Optimization of Two-stage High-voltage Electrostatic Separation Parameters for Retired Passenger Vehicle Plastics by Response Surface Methodology

HONGSHEN ZHANG*, GUANGHAO PAN, HONGFEI ZHENG
Kunming University of Science and Technology, Faculty of Mechanical and Electrical Engineering, No.727 South Jingming Rd., Chenggong District, Kunming, 650500, China

Abstracts: *Plastic parts in retired passenger vehicles are derived from non-renewable oil resources, and recycling them can conserve energy and reduce the burden on the environment. Effective separation is the premise of recycling vehicle plastics, and electrostatic separation is a clean and efficient method of plastic separation. On the basis of a self-developed, two-stage electrostatic separation equipment, this study investigated the high-voltage electrostatic separation of polyamide (PA), polyethylene (PE), and polypropylene (PP) mixtures. First, the single-factor experiment method was used to explore the influence of voltage, electrode spacing, and electrode inclination angle on the separation results. Second, the response surface methodology was employed to comprehensively analyze the effects of voltage, electrode spacing, and electrode inclination angle on the recovery rates of the three particles and their interactions. The optimum parameters for the secondary electrostatic separation of the three particles were determined to be 44 kV voltage, 156 mm electrode spacing, and 10° electrode inclination. Experimental verification showed that after the two-stage, electrostatic separation device was optimized through the response surface methodology, the purity of the PA particles reached 98.56%, and the recovery rate reached 96%. The purity of the PP particles reached 81.93%, and the recovery rate was 87.5%. Meanwhile, the purity of the PE particles reached 86.11%, and the recovery rate was 73%. This research provides a reference for the multi-stage, high-voltage, electrostatic separation of various automotive plastic particles.*

Keywords*: Retired passenger vehicles; plastic waste; multistage electrostatic separation; response surface methodology; optimal parameters*

1. Introduction

China's automobile industry is developing rapidly and has ranked first in the world for 13 consecutive years. At the end of 2021, the number of cars exceeded 300 million [1]. The increase in car ownership has led to the rapid growth of car scrap, which means a large amount of car waste enters the recycling stage [2]. Plastic polymer is a polymer material formed by the polymerization of petroleum products. It has the characteristics of light weight, easy forming, corrosion resistance, weather resistance, and insulation, so it is widely used in automotive interior, exterior, and functional structural parts. Retired vehicles contain a wide range of plastic polymers, and the weight of plastic polymers for a common vehicle has increased from 6% in 1970 to 16% in 2010 [3]. Various plastic parts in scrapped vehicles are processed by polymer materials formed by the polymerization of petroleum products, which contain abundant non-renewable petroleum resources. If these plastics are not subjected to effective centralized processing, they will cause a massive waste of resources, and the inflow into the environment will exert great damage on the ecological environment [4].

The commonly used separation methods for plastic polymers mainly include manual separation, gravity separation, density flotation, spectral separation, and electrostatic separation [5]. Manual separation is time consuming and laborious and has poor efficiency and separating effect. Gravity separation cannot separate plastic polymers with the same specific gravity, and density flotation consumes much water, has a complicated procedure, and requires drying of the separated results.

email: hongshen@kust.edu.cn

Meanwhile, spectral separation is minimally effective in recognizing polymer materials with dark or similar colors. Electrostatic separation, one of the commonly used separation methods for plastic polymers, has attracted much attention due to its good separation effect and simple equipment [6-8].

Electrostatic separation technology combines the friction electric effect with electric field force and uses the surface charge characteristics of the friction material to make the insulation material charged in the appropriate device; afterward, the particles with positive and negative charges are introduced into the electric field, and the particles are separated by the action of the strong electric field according to the polarity of the material [9-11]. Electrostatic separators for plastic waste are being developed around the world to improve the efficiency of the separation process [12]. Electrostatic separation has attracted increasing attention in the field of plastic recovery due to its advantages of high efficiency, cleanness, simple equipment, absence of secondary pollution, and no need for dehydration of plastic materials [13,14]. Li et al. studied the charge properties of waste polymer particles in friction electrostatic separation through vibrating tribo-charging and cyclone tribo-charging and proved that cyclone tribo-charging is more effective and stable than vibrating tribo-charging, and its higher relative humidity hinders the charge effect [15]. Amar et al. used a simple mathematical model to simulate the separation results of binary mixed particle materials by using a friction air–electrostatic separator, and the calculation results were consistent with the experimental results [16].

Zhang et al. studied the friction electrostatic separation of polypropylene (PP) and acrylonitrile–butadiene–styrene (ABS) polymers of scrap passenger vehicles through high-voltage friction electrostatic separation technology. The experimental results showed that the separation rate of PP and ABS polymers exceeds 60%, and the pureness is more than 95% [17]. Li et al. developed an innovative recovery method called charge decay electrostatic separation. When they separated mixed polymer waste from a waste refrigerator, the pureness of polyvinyl chloride (PVC) reached 96%, and the recovery rate was 99% [18]. Li et al. proposed two modes of separating mixed polymer particles [19]. First, only one kind of particle is separated from the mixed particles at each time. Second, mixed particles are divided into two groups. Their separation results showed that the average separation efficiencies of the first and second modes are 72.44% and 65.18%, respectively. Rybarczyk et al. developed an effective method to evaluate the electrostatic separation quality of polymer mixtures by using a visual system. The experimental results showed that the visual system can be successfully applied to the study of polymer electrostatic separation [20]. Meanwhile, Ahlem et al. used three friction-charge devices to separate a mixture of PS (HIPS)/BFR-free HIPS, BFRPP/BFR-free PP, and BFRPE/BFR-free PE. The experiment proved that using electrostatic separation technology to separate mixtures containing bromine is feasible [21].

By referring to the theoretical basis of high-voltage electrostatic separation and computer simulation results, scholars have studied a series of electrostatic separation processes and developed various types of high-voltage electrostatic separators. Silveira et al. used a roller electrode to separate crushed waste. The experiment showed that the separation effect of friction high-voltage electrostatic separation on plastic is good, and the recovery rate and pureness exceed 90.2% [22]. Rezoug et al. studied an electrostatic separation device for recovering granular polymer materials. The separation results showed that the pureness of PVC, PC, and HDPE is 85%, 95%, and 75%, respectively, and the recovery rate is over 80% [23]. Djamel et al. developed a new propeller-type pneumatic friction charge device, which was used for a charge separation experiment on a ternary mixture. The recovery rate and pureness were above 90% [24]. Noureddine et al. studied the factors that affect the separation rate of WPVC particles with a size of 100 μm by using a fluidized bed friction electrostatic separation system. The results showed that high-pressure level, disk speed, fluidization rate, total mass of the fluidized bed, and particle mixture have significant indigenous effects on recovery rate and pureness [25]. Reriballah et al. developed a new four-cylinder electrostatic separator based on a free-falling separation system and conducted experiments on PVC and UPVC binary mixtures. The results showed that under the optimal control variables, the recovery rate and pureness of the separation products exceed 95% [26]. Rodrigues

et al. developed an electrostatic separation device for polymer waste based on airflow friction charging in a PVC tube; the device has high efficiency in separating the ternary mixture of PVC/HDPE/PET [27].

In summary, current research on electrostatic separation technology focuses on commodity and waste electrical and electronic equipment (WEEE) polymers. The research on electrostatic separation of vehicle polymers is insufficient, and the research on multi-stage separation is even rarer. The current study uses a self-developed, free-fall, electrostatic separation device to conduct a two-stage electrostatic separation experiment on three kinds of particles commonly used in passenger vehicles (i.e., PA, PP, and PE). The effects of voltage, electrode plate spacing, and electrode inclination on the separation effect are studied. The response surface methodology is used to explore the interaction of various factors, and the optimal parameters of separation pureness and separation recovery are obtained through optimization.

2. Materials and methods

2.1. Friction barrel-type charging mechanism

The study uses a friction barrel-type charging mechanism, as shown in Figure 1, whose material is PMMA (organic glass). To make the polymer particles fully charged, a uniform distribution of fins is set inside the friction bucket to increase the amount of friction. A three-phase asynchronous motor (power of 1.5 KW and working voltage of 380 V) is used as a power source, and belt and friction wheel drives are employed to drive the friction barrel's rotation. The speed and steering are changed by a frequency converter. During the working process, the particles enter the friction barrel through the feed port. With the rotation of the friction barrel, the collision between the particles and the friction barrel wall completes the charge.

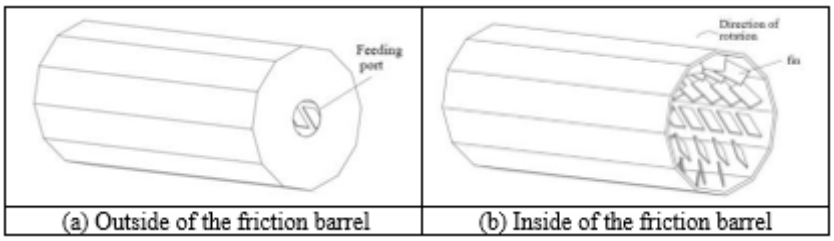

Figure 1. Friction barrel

2.2. Free-fall separation mechanism

The study adopts a self-developed, two-stage, free-fall electrostatic separation mechanism, whose equipment structure sketch is shown in Figure 2. The mechanism is composed of two superimposed free-fall separation systems with electrode plates made of 1060 pure aluminum. The electrode plates are connected to the electrostatic generator (0-100 kV, adjustable) to generate an electric field for controlling the trajectory deviation of the charged particles. The position and tilt angle of each electrode plate can be adjusted. When the separation mechanism works, the particles enter the high-voltage electric field through the blanking mouth, and the trajectory deviates under the action of electric field force, gravity, and other factors. Then, the particles fall into different collection tanks to realize the separation of mixed particles.

The other experimental equipment used in this study include an HS004 electrostatic generator, a Faraday cup, a Monroe Electronics 284 coulomb meter, temperature and humidity meters, and an electronic balance.

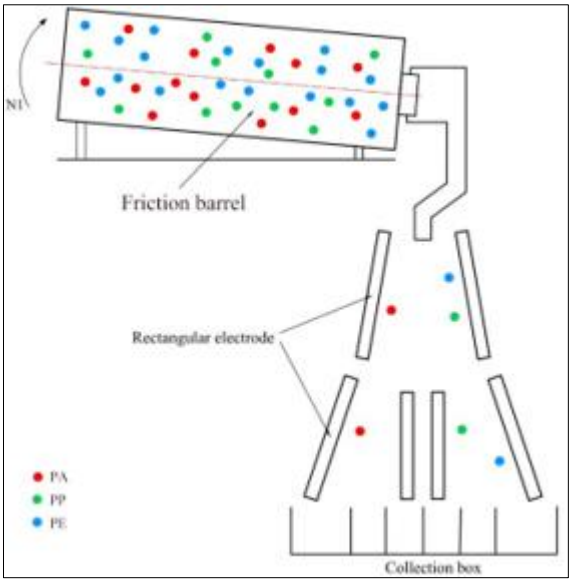

Figure 2. Structural sketch of the electrostatic separation equipment

2.3. Experimental materials

With the continuous improvement of polymer properties, polymer materials are widely used in the manufacturing of various interior decoration parts of automobiles and can now replace metal materials in the manufacturing of some structural, functional, and external parts. This material meets not only performance requirements, but also vehicle requirements on weight [28].

Common automotive polymers include PP, ABS, polyethylene (PE), PVC, polyamide (PA), and polyurethane (PU) [29]. In practical applications, most passenger car polymers are black. Distinguishing the separation effect through naked eyes is difficult because of the same color, size, and shape obtained after crushing. According to experimental results, the changes in the physical properties of a polymer in the production process can be ignored. Therefore, new polymers with a different appearance and color can be used as alternatives for electrostatic separation experiments. Several common automotive thermoplastic polymer feedstocks selected for this study are PA, PE, and PP pellets, and their morphology is shown in Figure 3. The above-mentioned particles differ significantly in morphology or color to facilitate the calculation of recovery rate and separation pureness after the separation experiments.

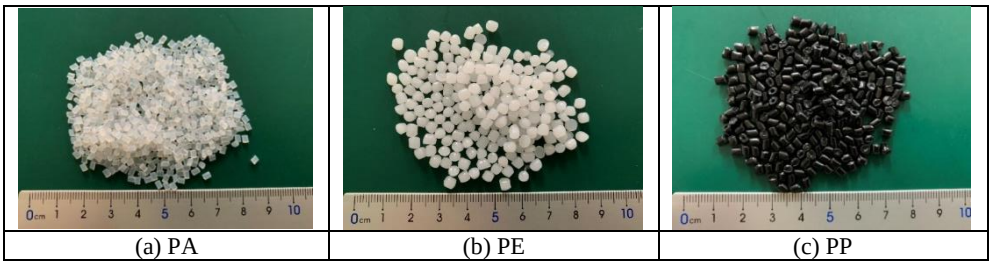

(a) PA (b) PE (c) PP

Figure 3. Experimental materials

3 Results and discussions

3.1. Factors that influence the electrostatic separation of polymer

The polymer enters the free-fall separation system for charging and separating after being charged in the friction barrel charging device. Figure 4 shows the parameters used in the secondary free-fall separation system, where d_0 is the top spacing of two electrode plates in the first-stage separator; θ_1 is the inclination angle of the first-stage electrode plate; U_1 is the voltage of the first-stage separator; L is

the length of an electrode plate; d_{21}, d_{22} is the distance between the two sides of the second-stage electrode plate and the top of the middle vertical electrode plate; θ_{21}, θ_{22} is the inclination angle of the second-stage electrode plate; U_{21}, U_{22} is the voltage of the second-stage separator; and h is the distance between two electrode plates.

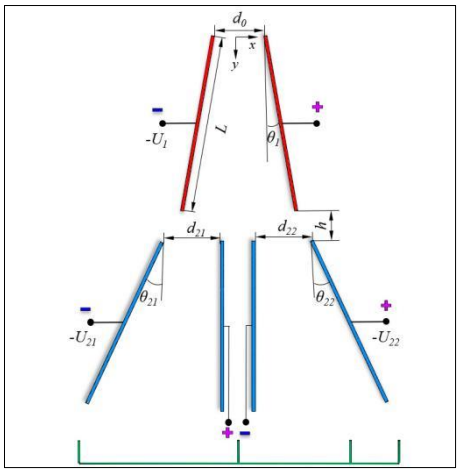

Figure 4. Two-stage separation parameters

In the free-falling separation system, the main factors that affect the electric field strength are voltage, electrode plate spacing, and electrode inclination. A voltage that is too small leads to insufficient electric field force on the particles and a shifted trajectory; a voltage that is too large leads to an excessive electric field force on the particles and early collision with the electrode plate, both of which result in a low separation rate. The electric field strength is inversely proportional to the electrode plate spacing, and a too large or too small a spacing leads to a low separation rate. The electrode inclination angle also has a great influence on the separation results. When the electrode plate is placed vertically, a uniform strong electric field is formed between the electrode plates, and the force on the horizontal direction of the particles is large, leading to changes in the trajectory of some particles and affecting the separation results; if the electrode plate inclination angle is too large, the electric field decays too fast, and the horizontal displacement of the particles is too small, thereby reducing the separation rate.

On the basis of the discussion above, this study conducts single-factor experiments on PA, PP, and PE particles to study the influence law of the influencing factors on the separation effect and the best application range.

3.2. Single-factor experiments and results of three kinds of particles

The PA, PP, and PE particles are mixed with 10 g each for frictional charging at an experimental temperature of 19°C-23°C and ambient relative humidity of $50 \pm 2\%$. After charging, the PA particles are positively charged and biased to the left electrode plate; both PP and PE particles are negatively charged and biased to the right electrode plate at the same time, but due to the different density and saturation charge of the two particles, the charge-to-mass ratio is different, leading to a difference in the horizontal offset distance of the two particles in the electric field.

The response surface method is then used to optimize the first-stage separation factors, and the optimal results are obtained. U_1 is set to 40 kV, θ_1 is set to 6°, d_0 is set to 115 mm, and h is set to 5 cm. The voltage U_2, electrode spacing d_2, and electrode inclination θ_2 of the second-stage electrode plate are tested via a single-factor test, and the following results are obtained.

(1) When electrode spacing d_2 is fixed to 175 mm and electrode inclination angle θ_2 is fixed to 15°, the separation experiments are carried out at separation voltages of 30, 40, and 50 kV. The experimental results are as follows. The pureness and recovery rate of the PA particles exceed 90% and increase with

the increase in voltage. The pureness and recovery of the PE particles decrease with the increase in voltage, and the pureness and recovery of the PP particles initially increase and then decrease with the increase in voltage.

(2) When separation voltage U_2 is fixed at 40 kV and electrode angle θ_2 is fixed at 15°, the separation experiments are carried out at electrode spacing d_2 of 150, 175, and 200 mm. The experimental results show that the pureness and recovery of the PA particles are close to 96% and basically remain unchanged. The pureness and recovery of the PP and PE particles decrease with the increase in spacing.

(3) When separation voltage U_2 is fixed to 40 kV and electrode spacing d_2 is fixed to 175 mm, the separation experiments are carried out when the inclination angles θ_2 of the electrode plates are 10°, 15°, and 20°. The experimental results show that the pureness and recovery rate of the PA particles are close to 96%, and they remain basically unchanged with the increase in the inclination angle. The pureness and recovery of the PP and PE particles decrease with the increase in the dip angle, but the decrease in the PE particles is small.

3.3. Optimization of influence parameters for mixed separation of three vehicle polymers

The single-factor experiment only considers the influence of one factor on the experimental results. The other factors are fixed, and the effects of each factor and multi-factor interaction on the experimental results cannot be determined. Response surface methodology (RSM) can visually observe the relationship between factors and response values and select the best conditions for the experimental design [30]. The Box–Behnken experimental design (BBD) does not have an axial point, so the safe operating region is not exceeded in practice [31]. As a result, the BBD method of the RSM method is used in this study to optimize the experimental parameters for the electrostatic sorting of the three particles.

After mixed charging of the PA, PP, and PE particles, the PA particles are positively charged, and the PP and PE particles are negatively charged. In the first-stage separation chamber, the PA particles enter the left second-stage separation chamber alone. Therefore, in the single-factor experiment, the pureness and recovery of the PA particles are close to 98%. In the response surface optimization experiment, only the pureness and recovery of the PP and PE particles are adopted as the response values, and secondary separation voltage U_2, electrode spacing d_2, and electrode inclination θ_2 are selected as the influencing factors. Table 1 shows the range and level of each influencing factor.

Table 1. Range and level of the influencing factors

Level	-1	0	1
A: voltage/kV	30	40	50
B: electrode spacing/mm	150	175	200
C: electrode inclination/°	10	15	20

3.4. Analysis of PP particle separation results

The experimental design scheme and the results of the optimization of the response surface for the PP particles are shown in Table 2.

The second-order regression equations, with PP particle pureness and recovery rate as the response values, are obtained by regression fitting as follows:

$$R_1 = 78.66 - 1.17A - 4.34B - 1.11C - 1.16AB + 1.36AC + 1.79BC - 1.64A^2 - 0.64B^2 + 0.32C^2,$$

$$R_2 = 85.60 - 2.50A - 4.13B - 1.63C + 0.50AB + 1.00AC + 2.25BC - 3.18A^2 - 0.93B^2 - 1.42C^2,$$

where R_1 and R_2 are the pureness and recovery of PP particles, respectively, and A, B, and C refer to voltage, electrode spacing, and electrode plate inclination, respectively. Tables 3 and 4 are variance analysis tables with the response values of PP pureness and recovery.

Table 2. Experimental design and results

No.	A: Voltage/kV	B: Electrode spacing/mm	C: Electrode inclination/°	Pureness of PP/%	Recovery rate of PP/%
1	30	200	15	75.27	79
2	50	200	15	69.44	75
3	50	175	10	76.8	79
4	40	200	10	72.7	79
5	30	175	20	75.14	81
6	50	150	15	79.81	83
7	40	200	20	74.67	80
8	40	175	15	78.45	86
9	40	175	15	77.19	84
10	40	175	15	79.85	88
11	40	175	15	79.52	84
12	40	150	20	80.39	83
13	50	175	20	76.69	78
14	30	150	15	81	89
15	40	175	15	78.29	86
16	30	175	10	80.7	86
17	40	150	10	85.6	91

As indicated in Tabs. 3 and 4, the *F* values of the response surface optimization models for the pureness and recovery of the PP particles are 18.74 and 18.21, respectively, indicating that the two response surface models used to optimize the pureness and recovery of PP particles have high confidence. The P values are less than 0.001, showing that the fitted regression models used are highly significant and can simulate the actual situation. Meanwhile, the *F* and P values of the lack-of-fit terms of both models are greater than 0.05, indicating that the out-of-fit factors have a small effect on the results. The coefficients of determination of both models show that the models can reveal 96.02% and 95.90% of the response values. The signal-to-noise ratio of both models is greater than 4, indicating a high degree of fit.

Table 3. ANOVA table with response values for PP pureness

Source	Sum of squares	Df	Mean square	*F*-value	P-value	Significance level
Model	211.01	9	23.45	18.74	0.0004	significant
A	10.79	1	10.97	8.77	0.0210	
B	150.68	1	150.68	120.47	＜0.0001	
C	9.92	1	9.92	7.93	0.0259	
AB	5.38	1	5.38	4.30	0.0767	
AC	7.43	1	7.43	5.94	0.0450	

BC	12.89	1	12.89	10.30	0.0149	
A^2	11.38	1	11.38	9.10	0.0195	
B^2	1.70	1	1.70	1.36	0.2813	
C^2	0.42	1	0.42	0.34	0.5799	
Residual	8.76	7	1.25			
Lack of fit	4.26	3	1.42	1.26	0.2409	not significant
Pure error	4.50	4	1.12			
Cor Total	219.77	16				

Note: $P < 0.01$ is highly significant; $P < 0.05$ is significant; $P > 0.05$ is not significant.

Table 4. ANOVA table with response values as PP recoveries

Source	Sum of squares	Df	Mean square	*F*-value	P-value	Significance level
Model	291.55	9	32.39	18.21	0.0005	significant
A	50.00	1	50.00	28.11	0.0011	
B	136.12	1	136.12	76.54	＜0.0001	
C	21.13	1	21.13	11.88	0.0107	
AB	1.00	1	1.00	0.56	0.4778	
AC	4.00	1	4.00	2.25	0.1774	
BC	20.25	1	20.25	11.39	0.0119	
A^2	42.44	1	42.44	23.86	0.0018	
B^2	3.60	1	3.60	2.03	0.1977	
C^2	8.55	1	8.55	4.81	0.0644	
Residual	12.45	7	1.78			
Lack of fit	1.25	3	0.42	0.15	0.9253	not significant
Pure error	11.20	4	2.80			
Cor Total	304.00	16				

Note: $P < 0.01$ is highly significant; $P < 0.05$ is significant; $P > 0.05$ is not significant.

The ANOVA conducted with the pureness of the PP pellets as the response value reveals that factor B has a highly significant effect on the pureness of the PP pellets. Factors A, C, AC, BC, and A^2 have a significant effect on the pureness of the PP pellets, and factors AB, B^2, and C^2 have a non-significant effect on the pureness of the PP pellets. The significant effects of the three variable factors on the pureness of the PP particles can be ordered as follows in terms of significance: electrode spacing, electrode inclination angle, and voltage. The ANOVA conducted with PP particle recovery as the response value shows that electrode spacing has the most significant effect on PP particle recovery among the three influencing factors, and the interaction between electrode spacing and electrode inclination has the most significant effect on PP particle recovery. The significant effects of the three variable factors on the recovery of PP particles can be ordered as follows in terms of significance: electrode spacing, voltage, and electrode inclination.

Figure 5 shows a 3D response surface diagram of the effect of the interaction of the three variable factors on the pureness of the PP particles. The steepness of the surface formed by the edges and top of the response surface reflects the significance of each factor on the response value. The steeper the slope is, the more obvious the impact is on the response value; the gentler the slope is, the smaller the impact is. The figure also shows that the smaller the electrode inclination angle is, the higher the pureness of

PP particles is. When the voltage is 35-45 kV and the electrode spacing is 150 mm, the pureness of the PP particles is high.

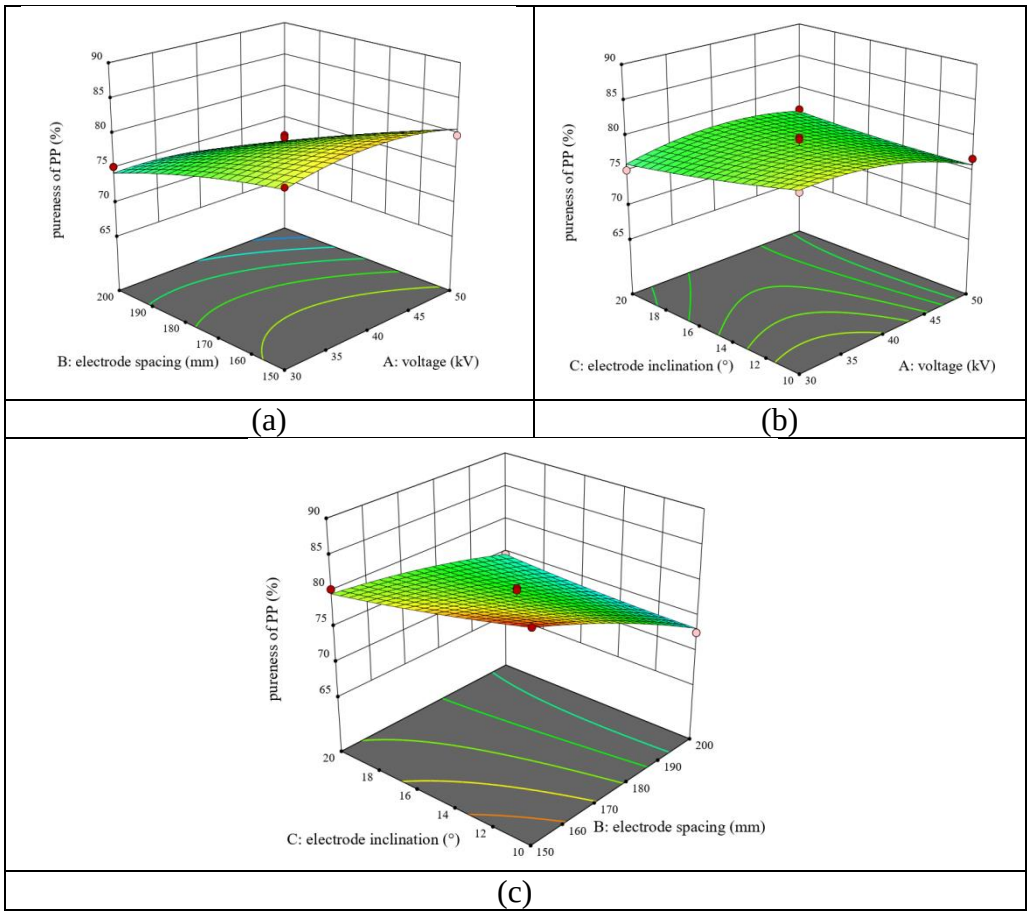

Figure 5. Effect of interactions on the pureness of PP particles

Figure 6 shows a 3D response surface plot of the three influencing factors on the recovery rate of the PP particles. The results show that voltage and electrode spacing are important factors that affect the recovery rate of PP, and the voltage must be controlled within 35–45 kV to obtain a high recovery rate.

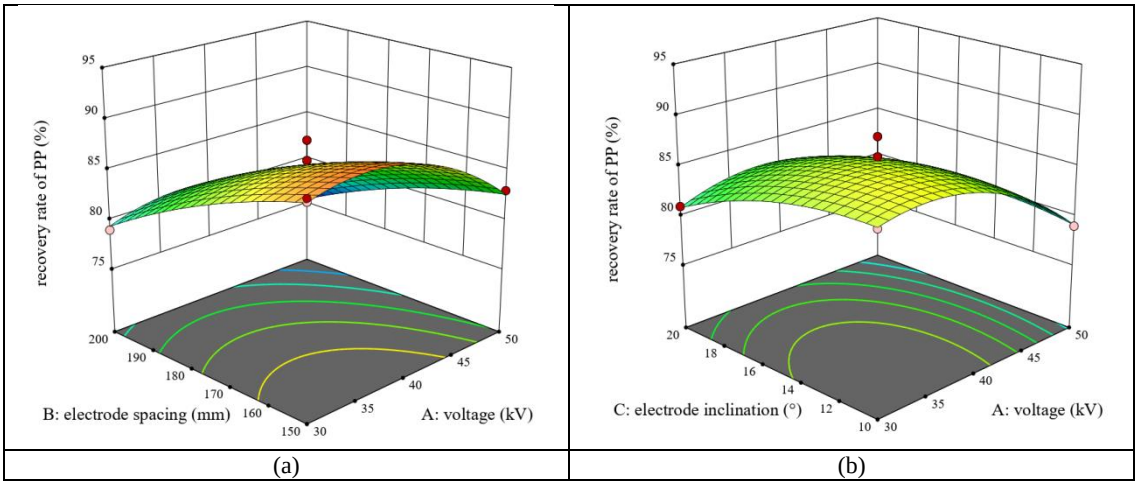

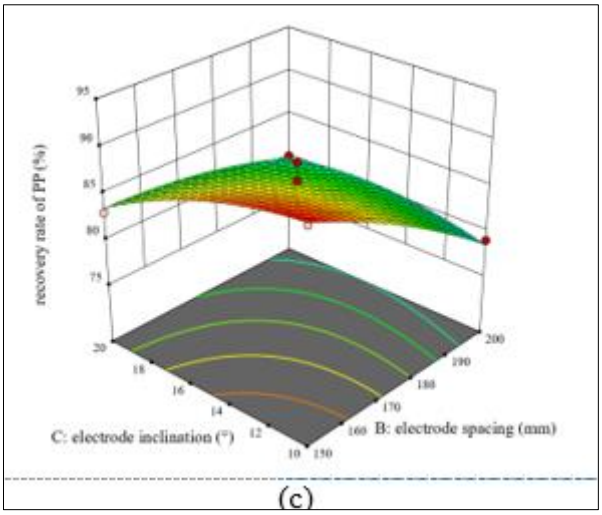

Figure 6. Effect of interaction on the recovery of PP particles

3.5. Analysis of PE particle separation results

The experimental design scheme and the results of the optimization of the response surface for PE particles are shown in Table 5.

Table 5. Experimental design and results

No.	A: voltage/kV	B: electrode spacing/mm	C: electrode inclination/°	Pureness of PE/%	Recovery rate of PE/%
1	40	175	15	80.92	79
2	50	200	15	78.48	79
3	50	175	10	88.05	80
4	30	150	15	82.11	62
5	30	200	15	80.14	63
6	40	150	10	86.46	68
7	50	175	20	80.65	69
8	40	150	20	82.44	60
9	40	200	10	80.01	71
10	40	175	15	82.69	81
11	40	175	15	82.89	78
12	40	175	15	82.06	81
13	40	175	15	78.95	83
14	30	175	10	81	65
15	40	200	20	77.29	69
16	50	150	15	86.93	68
17	30	175	20	81.5	65

The second-order regression equations with PE particle pureness and recovery rate as the response values are obtained by regression fitting as follows:

$$R_1 = 81.50 + 1.17A - 2.75B - 1.70C - 1.62AB - 1.97AC + 0.32BC + 0.83A^2 - 0.42B^2 + 0.47C^2,$$

$$R_2 = 80.40 + 5.13A + 3.00B - 2.63C + 2.50AB - 2.75AC + 1.50BC - 4.83A^2 - 7.58B^2 - 5.82C^2,$$

where R_1 and R_2 are the pureness and recovery of PE particles, respectively, and A, B, and C refer to voltage, electrode spacing, and electrode plate inclination. Tables 6 and 7 are variance analysis tables with the response values of PP pureness and recovery.

Table 6. ANOVA table with response values for PE pureness

Source	Sum of squares	Df	Mean square	*F*-value	P-value	Significance level
Model	125.86	9	13.98	8.27	0.0054	significant
A	10.95	1	10.95	6.48	0.0384	
B	60.61	1	60.61	35.85	0.0005	
C	23.26	1	23.26	13.76	0.0076	
AB	10.50	1	10.50	6.21	0.0415	
AC	15.60	1	15.60	9.23	0.0189	
BC	0.42	1	0.42	0.25	0.6325	
A^2	2.91	1	2.91	1.72	0.2308	
B^2	0.74	1	0.74	0.44	0.5301	
C^2	0.92	1	0.92	0.54	0.4855	
Residual	11.83	7	1.69			
Lack of fit	1.33	3	0.44	0.17	0.9119	not significant
Pure error	10.50	4	2.63			
Cor Total	137.69	16				

Note: $P < 0.01$ is highly significant; $P < 0.05$ is significant; $P > 0.05$ is not significant.

Table 7. ANOVA table with response values as PP recoveries

Source	**Sum of squares**	**Df**	**Mean square**	***F*-value**	**P-value**	**Significance level**
Model	938.02	9	104.22	44.35	< 0.0001	significant
A	210.13	1	210.13	89.41	< 0.0001	
B	72.00	1	72.00	30.64	0.0009	
C	55.13	1	55.13	23.46	0.0019	
AB	25.00	1	25.00	10.64	0.0138	
AC	30.25	1	30.25	12.87	0.0089	
BC	9.00	1	9.00	3.83	0.0915	
A^2	98.02	1	98.02	41.71	0.0003	
B^2	241.60	1	241.60	102.81	< 0.0001	
C^2	142.87	1	142.87	60.79	0.0001	
Residual error	16.45	7	2.35			
Lack of fit	1.25	3	0.42	0.11	0.9500	not significant
Pure error	15.20	4	3.80			
Cor Total	954.47	16				

Note: $P < 0.01$ is highly significant; $P < 0.05$ is significant; $P > 0.05$ is not significant.

As shown in Tables 6 and 7, the *F* values of the response surface optimization models for the pureness and recovery of PE particles are 8.27 and 44.35, respectively, indicating that the two response surface models used to optimize the pureness and recovery of PE particles have high confidence. The P values are less than 0.001, indicating that the fitted regression models used are highly significant and can simulate the actual situation. Meanwhile, the *F* and P values of the lack-of-fit terms of both models are greater than 0.05, indicating that the out-of-fit factors have a small effect on the results. The coefficients of determination of both models indicate that the models can reveal 91.41 and 98.28% of the response values. The signal-to-noise ratio of both models is greater than 4, which is associated with a high degree of fit.

According to the ANOVA with PE pellet pureness as the response value, the significant effects of the three variable factors on PE pellet pureness are in the following order: electrode spacing, electrode inclination, and voltage. According to the ANOVA with PE pellet recovery as the response value, the significant effects of the three variable factors on PE pellet recovery are in the following order: voltage, electrode spacing, and electrode inclination.

Figure 7 presents a 3D response surface diagram of the influence of the three variable factors on the pureness of PE particles. According to Figure 7, when the electrode angle is fixed, the pureness of PE particles decreases with the increase in voltage and electrode spacing. When the electrode spacing is fixed, the pureness of PE particles decreases with the increase in voltage and electrode inclination. When the voltage is fixed, the pureness of PE particles gradually decreases with the increase in electrode inclination and electrode spacing.

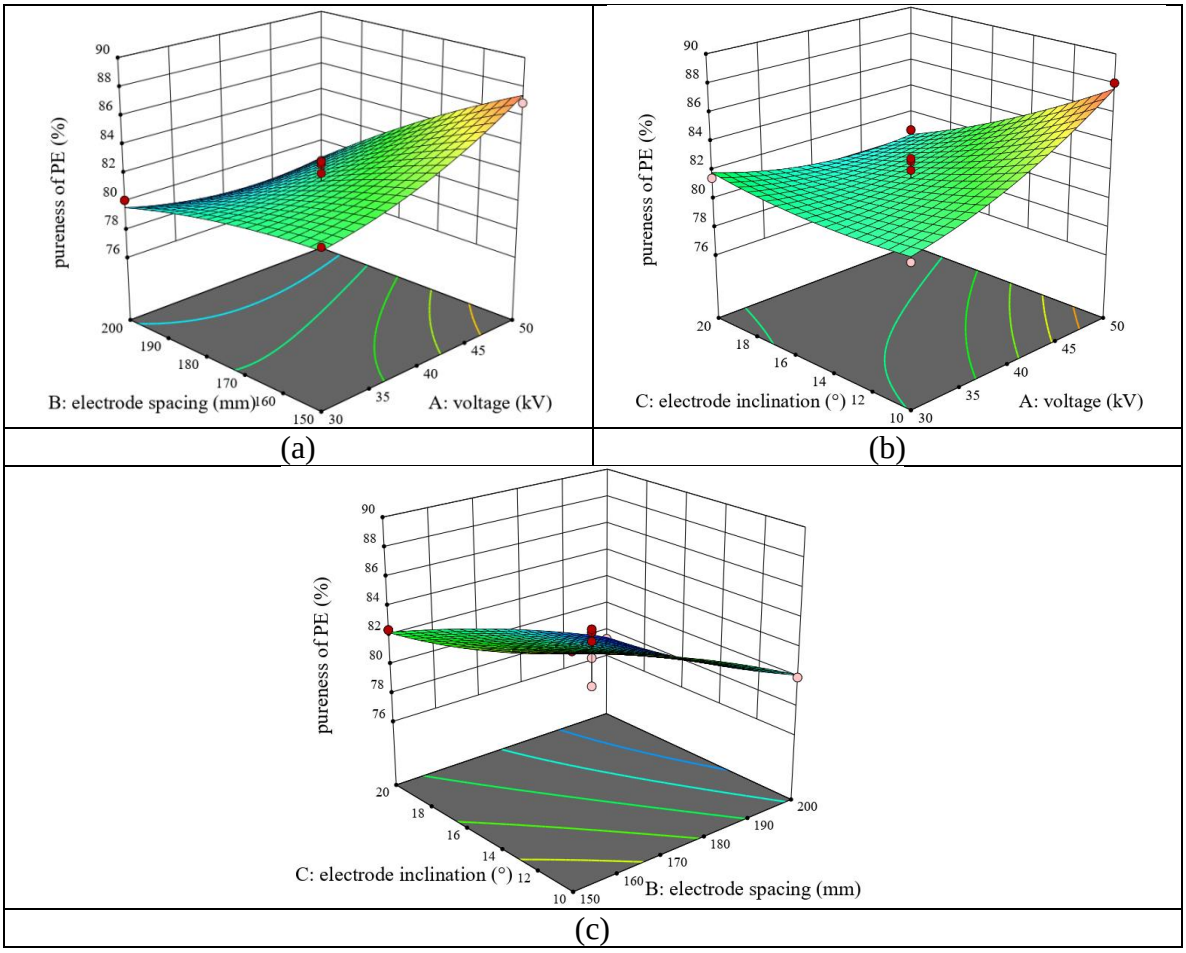

Figure 7. Effect of interactions on the pureness of PE particles

Figure 8 shows a 3D response surface diagram of the three influencing factors on the recovery rate of PE pellets. When the electrode inclination angle is fixed, the recovery rate of PE pellets increases then

decreases with the increase in voltage and electrode inclination angle. The suitable values are voltage of 40-50 kV and electrode inclination angle of 170-190 mm. The condition with voltage of 40-50 kV and electrode inclination angle of 12°-16° is likewise suitable. When the voltage is fixed, the recovery rate of PE particles also increases then decreases with the increase in electrode pitch and electrode inclination angle. The recovery rate is high when the electrode pitch is 170-190 mm and the electrode inclination angle is 12°-16°.

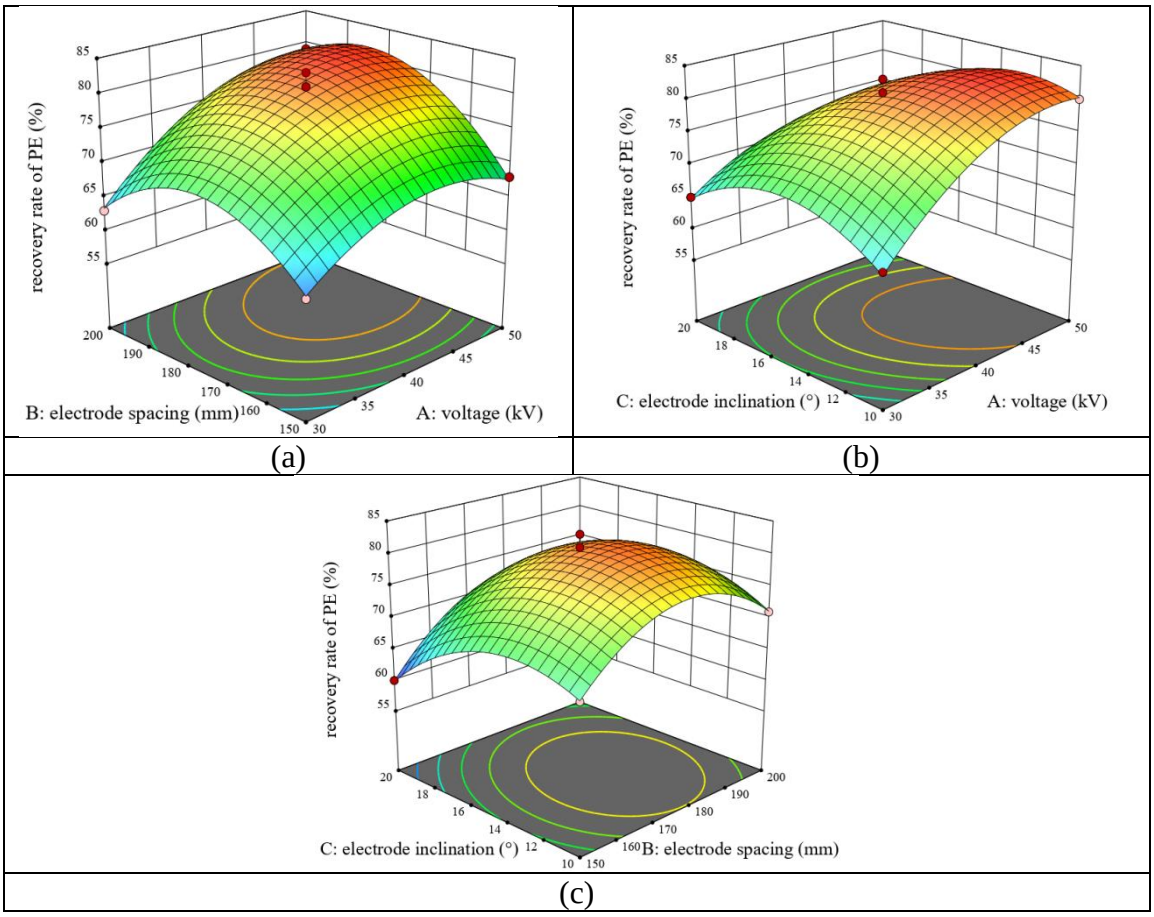

Figure 8. Effect of interaction on the recovery of PP particles

3.6. Optimum parameters optimized by RSM

This study also verifies the accuracy of the response surface optimization model in predicting the secondary sorting results and obtains the optimal values of each variable. The optimal sorting parameters obtained from the analysis of Design Expert 13 software are as follows: 43.682 kV for voltage, 155.973 mm for electrode spacing, 10° for electrode tilt angle, 83.560% for PP pellet pureness, and 88.257% for PP pellet recovery. The predicted pureness of PP particles is 83.560%, and the predicted recovery is 88.257%; meanwhile, the predicted pureness of PE particles is 87.498%, and the predicted recovery is 73.215%. In the actual experiment, the voltage is set to 44 kV, the electrode spacing is set to 156 mm, and the electrode inclination angle is set to 10°. Table 8 shows the experimental results of the secondary sorting optimization, which verifies the reliability of the model.

Table 8. Optimization of the validation experimental results

Particle type	Predicted value	Actual value
Pureness of PP particles	83.560%	81.93%
Recovery rate of PP particles	88.257%	87.5%

Pureness of PE particles	87.498%	86.11%
Recovery rate of PE particles	73.215%	73%

4. Conclusions

With the increase in car ownership, car scrap is also increasing annually. However, electrostatic separation of automobile waste polymer particles mostly adopts unipolar separation, and the research on multi-stage separation is lacking.

In this study, a secondary high-voltage electrostatic separation experiment was conducted on PA/PP/PE mixed particles by using a two-stage, free fall, separation device. The single-factor experiment method was used first, and the response surface experiment method was employed afterward to analyze the influence of the interaction of electrostatic separation voltage, electrode plate spacing, and electrode plate inclination angle on the separation pureness and recovery rate. After analysis, the following conclusions were derived:

- In the free-falling sorting system, the main factors that affected the electric field strength were voltage, electrode plate spacing, and electrode inclination. When the electric field intensity was too high or too low, the separation effect was changed, and the separation recovery rate and separation pureness were reduced.

- The influence of the three variable factors on the pureness of PP particles was in the following order: electrode spacing, electrode angle, and voltage. The significant influence on the recovery rate of PP particles was as follows: electrode spacing, voltage, and electrode inclination. The significant influence on the pureness of PE particles was as follows: electrode spacing, electrode inclination, and voltage. Lastly, the significant influence on the recovery rate of PE particles was as follows: voltage, electrode spacing, and electrode inclination.

- The optimal process parameters of secondary separation were voltage of 44 kV, electrode spacing of 156 mm, and electrode inclination of 10°. Under this condition, after the secondary separation of PA/PP/PE mixed particles, the pureness of PA particles reached 98.56%, and the recovery rate was 96%. The pureness of PP particles was 81.93%, and the recovery rate was 87.5%. Meanwhile, the pureness of PE particles was 86.11%, and the recovery rate reached 73%.

This study shows that three automotive plastics can be successfully separated by using secondary high-pressure electrostatic separation technology. The findings provide a reference for multi-stage electrostatic sorting of multiple retired passenger vehicle plastics.

AcknowledgementsThe authors express sincere thanks to the National Natural Science Foundation of China for financing this research within the project “Study on the mechanism of green high voltage electrostatic separation for ELV polymer particles” under the label 52065034.

References

1. ***Ministry of Public Security of the People's Republic of China-The national motor vehicle fleet will reach 395 million in 2021, with a 59.25% year-on-year increase in new energy vehicles, 2022. Available online: http://www.gov.cn/xinwen/202201/12/content_5667715.htm(accessed on 06. 08. 2022)

2. ZHANG H., ZHENG H., Artificial and natural aging of polypropylene used in passenger vehicle bumpers, *Mater. Plast.*, **58**(2), 2021, 201-210
2021, 201-210. https://doi.org/10.37358/MP.21.2.5492

3.KOZDERKA, M., ROSE, B., BAHLOULI, N., Recycled high impact polypropylene in the automotive industry - mechanical and environmental properties, *International Journal on Interactive Design and Manufacturing*, **11**(3), 2017, 737-750. DOI: 10.1007/s12008-016-0365-9

4.MENESES, R.A.M., CABRERA-PAPAMIJA, G., MACHUCA-MARTÍNEZ, F., RODRÍGUEZ L.A., DIOSA J.E., MOSQUERA-VARGAS, E., Plastic recycling and their use as raw material for the synthesis of carbonaceous materials, *Heliyon*, **8**(3), 2022, e09028.
https://doi.org/10.1016/j. heliyon.2022.e09028
5. QIN Y., YAO Z., RUAN J., XU Z., Motion Behavior Model and Multistage Magnetic Separation Method for the Removal of Impurities from Recycled Waste Plastics, *ACS Sustainable Chemistry & Engineering*, **9**(32), 2021, 10920-10928. https://doi.org/10.1021/acssuschemeng.1c03580
6. SHI J., ZHAO X., ZHANG Z., BAI X., XU Y., WANG H., ZHANG T., Theoretical and experimental study on the triboelectric separation of ternary plastics combination using fluidized bed, *Journal of Material Cycles and Waste Management*, **23**(6), 2021,2297-2306.
https://doi.org/10.1007/s10163-021-01296-3
7.LI T., YU D., ZHANG H., Triboelectrostatic separation of polypropylene, polyurethane, and polyvinylchloride used in passenger vehicles, *Waste Management*, **73**, 2018, 54-61.
https://doi.org/10.1016/j.wasman.2017.12.008
8.TIAN C., ZHANG H., ZHENG H., Kinematic analysis of particle movement in friction barrel-type tribocharger, *Journal of Mechanical Science and Technology*, **36** (7), 2022, 3301-3312.
DOI: 10.1007/s12206-022-0610-z
9.OLIVEIRA, C.M., BELLOPEDE, R., TORI, A., Study of Metal Recovery from Printed Circuit Boards by Physical-Mechanical Treatment Processes, *Materials Proceedings*, **121**(5), 2021.
https://doi.org/10.3390/materproc2021005121.
10.BOUKHOULDA, M.F., REZOUG, M.M., AKSA, W., MILOUDI, M., MEDLES, K., Triboelectrostatic separation of granular plastics mixtures from waste electric and electronic equipment, *Particulate Science and Technology*, **35**(5), 2017, 621-626.
https://doi.org/10.1080/02726351. 2017.1347226
11. ZHU H., TANG H., CHENG Y., Electrostatic separation technology for obtaining plant protein concentrates: A review, *Trends in Food Science & Technology*, **113**(6039), 2021,66-76.
https://doi.org/10.1016/j.tifs.2021.04.044
12. REGULSKI, R., CZARNECKA-KOMOROWSKA, D., JEDRYCZKA, C., Automated test bench for research on electrostatic separation in plastic recycling application, *Polska Akademia Nauk*, **69**(2), 2021, e136719. DOI: 10.24425/bpasts.2021.136719
13.BENAOUDA, I., ZEGHLOUL, T., MEDLES, K., *Insulating conveyor-belt-type electrostatic separator for triboelectrically-charged granular plastic wastes*., 2019 IEEE Industry Applications Society Annual Meeting, p.0958.
14.BOUTEFFAHA, A., BENDAOUD, A., REGUIG, A., Effects of the grid geometry on the performances of a triode-type corona electrode system, *Journal of Electrostatics*, **101**(C), 2019,103367.
https://doi.org/10.1016/j.elstat.2019.103367
15. LI J., WU G., XU Z., Tribo-charging properties of waste plastic granules in process of tribo-electrostatic separation, *Waste Management*, 35(1), 2015, 36-41.
https://doi.org/10.1016/j.wasman.2014.10.001
16. MIMOUNI, C., TILMATINE, A., RAHOU, F.Z., Numerical simulation of a tribo-aero-electrostatic separation of a ternary plastic granular mixture, *Journal of Electrostatics*, **88**, 2017, 2-9.
https://doi.org/10.1016/j.elstat.2017.01.015
17. ZHANG H., CHEN M., Triboelectrostatic separation for PP and ABS plastics in end of life passenger vehicles, *Journal of Material Cycles and Waste Management*, **19**(2), 2017, 884-897.
DOI 10.1007/s10163-016-0490-3
18. LI J., GAO K., XU Z., Charge-decay electrostatic separation for removing Polyvinyl chloride from mixed plastic wastes, *Journal of Cleaner Production*, **157**(20), 2017, 148-154.
https://doi.org/10.1016/j.jclepro.2017.03.233Get rights and content
19. LI J., XU Z., Compound tribo-electrostatic separation for recycling mixed plastic waste, *Journal of Hazardous Materials*, **367**, 2019, 43-49. https://doi.org/10.1016/j.jhazmat.2018.12.017

20. RYBARCZYK, D., JEDRYCZKA, C., REGULSKI, R., Assessment of the electrostatic separation effectiveness of plastic waste using a vision system, *Sensors*, **20**(24), 2020,7201. https://doi.org/10.3390/s20247201
21. BENABDERRAHMANE, A., MEDLES, K., ZEGHLOUL, T., RENOUX, P., DASCALESCU, L., PARENTY, A., Triboelectric Charging and Electrostatic Separation of Granular Polymers Containing Brominated Flame Retardants, *IEEE Transactions on Industry Applications*, **57**(1), 2021, 915-922. DOI: 10.1109/tia.2020.3031579
22. SILVEIRA, A.V.M., SANTANA, M.P., BERTUOL, D.A., Recovery of valuable materials from spent lithium ion batteries using electrostatic separation, *International Journal of Mineral Processing*, **169**, 2017, 91-98. https://doi.org/10.1016/j.minpro.2017.11.003
23. REZOUG, M., OUIDDIR, R., AKSA, W., Tribo-aero-electrostatic separator for ternary mixtures of granular plastics, *IEEE Transactions on Industry Applications*, **51**(2), 2015, 1161-1167. DOI: 10.1109/TIA.2014.2347451
24. FEKIR, D.E., MILOUDI, M., MILOUA, F., MEDLES, K., DASCALESCU, L., New propeller-type tribocharging device with application to the electrostatic separation of granular insulating materials, *IEEE Transactions on Industry Applications*, 53(3), 2017, 2416-2422. DOI**:** 10.1109/TIA.2017.2647802
25. BOUHAMRI, N., ZELMAT, M.E., TILMATINE, A., Micronized plastic waste recycling using two-disc tribo-electrostatic separation process, *Advanced Powder Technology*, **30**(3), 2019, 625-631. https://doi.org/10.1016/j.apt.2018.12.012
26. RERIBALLAH, H0, AKSA, W., TOUHAMI, S., Experimental modeling and optimization of a free-fall electrostatic separator equipped with four rotating-cylinder electrodes, *IEEE Transactions on Industry Applications*, **56**(5), 2020, 5472-5479. DOI: 10.1109/TIA.2020.3007126
27. RODRIGUES, B.M., SARON, C., Electrostatic separation of polymer waste by tribocharging system based on friction with PVC, *International Journal of Environmental Science and Technology*, **19**, 2022, 1293-1300. https://doi.org/10.1007/s13762-021-03229-x
28. GODARA, S.S., NAGAR, S.V., Analysis of frontal bumper beam of automobile vehicle by using carbon fiber composite material, *Materials Today: Proceedings*, **26**(2), 2020, 2601-2607. https://doi.org/10.1016/j.matpr.2020.02.550
29. SANZ, V.M., SERRANO, A.M., SCHLUMMER, M., A mini-review of the physical recycling methods for plastic parts in end-of-life vehicles, *Waste Management & Research*, **40**(12), 2022. http://dx.doi.org/10.1177/0734242x221094917
30. IBERAHIM, N., SETHUPATHI, S., GOH, C.L., BASHIR, M.J.K., AHMAD, W., Optimization of activated palm oil sludge biochar preparation for sulphur dioxide adsorption-ScienceDirect, *Journal of Environmental Management*, **248**(C), 2019,109302. https://doi.org/10.1016/j.jenvman.2019.109302
31. ZHOU R., ZHANG M., LI J., ZHAO W., Optimization of preparation conditions for biochar derived from water hyacinth by using response surface methodology (RSM) and its application in Pb^{2+} removal, *Journal of Environmental Chemical Engineering*, **8**(5), 2020, 104198. https://doi.org/10.1016/j.jece.2020.104198

Manuscript received: 6.08.2022